# THE MINNESOTA GRADING SYSTEM USING FUNDUS AUTOFLUORESCENCE OF EYE BANK EYES: A CORRELATION TO AGE-RELATED MACULAR DEGENERATION (AN AOS THESIS)

BY Timothy W. Olsen MD

## ABSTRACT

*Purpose*: To establish a grading system of eye bank eyes using fundus autofluorescence (FAF) and identify a methodology that correlates FAF to age-related macular degeneration (AMD) with clinical correlation to the Age-Related Eye Disease Study (AREDS).

*Methods*: Two hundred sixty-two eye bank eyes were evaluated using a standardized analysis of FAF. Measurements were taken with the confocal scanning laser ophthalmoscope (cSLO). First, high-resolution, digital, stereoscopic, color images were obtained and graded according to AREDS criteria. With the neurosensory retina removed, mean FAF values were obtained from cSLO images using software analysis that excludes areas of atrophy and other artifact, generating an FAF value from a grading template. Age and AMD grade were compared to FAF values. An internal fluorescence reference standard was tested.

*Results*: Standardization of the cSLO machine demonstrated that reliable data could be acquired after a 1-hour warm-up. Images obtained prior to 1 hour had falsely elevated levels of FAF. In this initial analysis, there was no statistical correlation of age to mean FAF. There was a statistically significant decrease in FAF from AREDS grade 1, 2 to 3, 4 ($P < .0001$). An internal fluorescent standard may serve as a quantitative reference.

*Conclusions*: The Minnesota Grading System (MGS) of FAF (MGS-FAF) establishes a standardized methodology for grading eye bank tissue to quantify FAF compounds in the retinal pigment epithelium and correlate these findings to the AREDS. Future studies could then correlate specific FAF to the aging process, histopathology AMD phenotypes, and other maculopathies, as well as to analyze the biochemistry of autofluorescent fluorophores.

*Trans Am Ophthalmol Soc 2008;106:383-401*

## INTRODUCTION

For thousands of years, people around the world have tried to defy aging by using elixirs, potions, or various therapies that increase longevity or maintain the youthful functions of our bodies. Technology has now enabled a scientific and rational approach to studying aging disorders. Finding new ways to delay the cumulative effects of time on our bodies has become a rapidly expanding area of research, especially given the aging population. Certainly, the visual system is affected by aging. In vision research, our goal is not longevity, but improving the quality of life by maintenance of a functional visual system throughout the entire life span of an individual. A rational analysis and a better understanding of the aging process are important for the discovery of therapeutic strategies that minimize the effects of aging on the eye.

### BACKGROUND

Age-related macular degeneration (AMD) is the leading cause of vision loss and blindness in individuals over age 65 in the developed world.[1-13] Epidemiologic studies have shown that approximately 10% of individuals over age 65 and 28% aged 75 to 85 will develop signs of AMD.[10] According to statistics from the US census, nearly 10 million more US citizens will enter the "over 65" demographic in the next 20 years, thus identifying AMD as a public health epidemic in the United States. Researchers have shown that comorbidity (depression, hip fractures, institutionalization, and decreased life span) related to visual impairment contributes significantly to the public health impact of AMD.[14] A recent epidemiologic study has shown that the severity of early, high-risk clinical features is a strong predictor of progression to later stages of AMD.[12]

The Age-Related Eye Disease Study (AREDS) is a large, prospective, interventional trial that has provided highly valuable data regarding the natural history of various stages of AMD progression and the role of antioxidants and zinc in delaying progression.[15] The AREDS uses clinical definitions of the various stages of AMD that have been adopted from internationally accepted standard criteria. Standard definitions have been adopted in order to develop a grading system of eye bank eyes, postmortem, that uses these same criteria.[16] A scientific approach has been to utilize the wealth of epidemiologic and prospective data of the AREDS to correlate our proteomic analysis of early stages of AMD. The goal is to identify early biochemical pathways involved in pathologic aging. Indeed, most individuals do not develop AMD. Some develop AMD at an early age. We refer to this as normal vs pathologic aging, respectively. We've utilized the clinical features associated with higher risk of progression to end-stage AMD as defined by the AREDS in our analysis of eye bank eyes and carefully analyzed the proteomics involved in pathologic vs normal aging.[17-23]

Treatments for AMD continue to improve. Anti–vascular endothelial growth factor (anti-VEFG) agents represent a major advancement in improving the visual function for those affected by advanced stages of neovascular or exudative AMD.[24-26] Newer agents and combination therapies may eventually prove to be even more effective than monotherapy. Treatment of AMD at an earlier stage could eliminate, prevent, or delay the onset of more advanced stages. A major emphasis of current research is to identify changes that are occurring in the earlier stages of the disease process that will allow us to identify pathways for earlier counseling or intervention. Evidence from several investigators suggests that apoptotic cell death of the retinal pigment epithelium (RPE) is a

From the Department of Ophthalmology, Emory University, Atlanta, Georgia.

primary cellular mechanism involved in vision loss.[27-33] Similarly, oxidative tissue injury is believed to play a major role in this early pathogenesis of AMD.[21,34-38] Recently, the role of the innate immune system in the pathogenesis of AMD was supported by a strong association of advanced AMD with a variant in the gene coding for complement factor H.[39-43] Early dysfunction of the immune system may lead to premature aging of select tissues, such as the RPE.

Our ability to diagnose and initiate early treatments for this disorder, especially for those at higher risk, should help decrease the impact of this degenerative condition on our population. Imaging technology is improving rapidly and may be helpful to identify those individuals at higher risk for disease progression at earlier stages of the disease process. Fundus imaging of aging pigments such as lipofuscin (LF) with fundus autofluorescence (FAF) may permit early detection of at-risk individuals. Early detection will be more important as newer therapies evolve, especially therapies targeting early-stage disease. The benefits of early treatment are emphasized by the estimated impact of full implementation of the AREDS supplements for individuals at risk. Indeed, it has been calculated that if everyone in the United States were treated according to recommendations of the AREDS, over 300,000 individuals would avoid development of advanced AMD over the next 5 years.

## CURRENT THERAPIES

As mentioned, the anti-VEGF agents have made a significant impact on improving the visual function of individuals with the exudative forms of AMD (eAMD).[24-26,44] Choroidal neovascularization (CNV) in eAMD accounts for most of the severe vision loss associated with advanced AMD. However, data from both the Beaver Dam Eye Study (BDES)[7] and the AREDS suggest that the rate of atrophic AMD (aAMD) represents approximately 30% of advanced AMD (AREDS: 257 developed central geographic atrophy (GA) vs 592 with CNV in 6.3 years, category 3 and 4[15]; BDES: 34 eyes with pure GA vs 77 eyes with eAMD out of 111 eyes with advanced AMD.[7]). The use of antioxidant vitamins has been shown to decrease the progression to advanced AMD by 25% over 5 years.[15] Despite the therapeutic advances, there are drawbacks. First, anti-VEGF therapy addresses the end stage of the disease process. Clearly, the primary mechanism involved in the pathogenesis of AMD is not due to excess VEGF production. Rather, VEGF is the result of complex biochemical events (hypoxia, inflammation, or other biochemical cascades) that lead to angiogenesis (eAMD) or apoptosis (aAMD) or some combination of these events. Again, an important concept of this work is to identifying early biochemical events in the pathogenesis of AMD that will lead to better preventative therapy, specifically, before the end-stage events such as angiogenesis and apoptosis occur.

## PROTEINS AND AGING

Proteins represent the building blocks of our cells and are the end product of our genome. Proper cellular function is highly dependent on proteins. After a protein is translated from messenger RNA (mRNA), it undergoes posttranslational folding that determines function and viability. Proper synthesis, folding, assembly, translocation, and clearance are essential. Altered protein formation or folding, due to a variety of mechanisms, may lead to a proteotoxic state and a cascade of molecular events leading to cell dysfunction or cell death. Other neurodegenerative diseases, such as Alzheimer disease and Parkinson disease, involve pathologic intracellular and extracellular protein aggregates. For example, Alzheimer disease is associated with accumulation of the small beta-amyloid peptide and the microtubule binding protein tau.[45] Targeting the protein turnover pathways allows investigators an earlier therapeutic window and, potentially, a more preventative approach to protein depositional diseases. Improving protein turnover (for example, the ubiquitin-proteasome pathway) could delay or inhibit a proteotoxic environment.[46,47]

Recently, the effects of aging on cellular proteins in the neurosensory retina and RPE have been established using high-throughput proteomic strategies on carefully graded human tissue.[17-23] Specific analysis is linked to a clinical grading system of eye bank eyes with AMD and establishes a direct link to large epidemiologic studies using similar definitions, such as the AREDS and the BDES. The system is referred to as the Minnesota Grading System (MGS).[16] Using MGS tissue, identification of specific protein states at each stage of the disease is possible by using mass-spectrometric analysis. Acquired data are then referenced to a large database of known proteins (available at www.matrixscience.com). Implications from proteomic analysis have direct links to the clinical stages of AMD. Indeed, one of the greatest limitations in current research of AMD is the lack of an animal model. The MGS allows for a noninterventional model of the true human condition of AMD.

## LIPOFUSCIN AND AUTOFLUORESCENCE

Lipofuscin represents a heterogeneous accumulation of oxidized proteins and lipids that increases within the lysosomes of postmitotic cells with age.[48-50] Studies using fluorescent microscopic techniques have shown that FAF is largely derived from LF within the RPE.[48,49,51] Lipofuscin is believed to originate from incompletely digested photoreceptor outer segment discs.[50,52] Specifically, N-retinylidene-N-retinylethanolamine (A2-E) has been identified as a major fluorophore in LF from human RPE.[53,54] Studies of human RPE cells in culture, loaded with an A2-E coupled to low-density lipoprotein, demonstrated accumulation of A2-E almost exclusively in the lysosomal compartment. These cells demonstrated strong inhibition of glycosaminoglycan catabolism, perturbation of the acidic intralysosomal milieu, and diminished hydrolase action with accumulation of undegraded material.[55] Many investigators have suggested a potential toxicity to the RPE from LF.[37,55-66] Interestingly, the association of LF to AMD[67-76] and to drusen[75,77-79] is highly variable. Smith and colleagues[75] recently suggested that there is an association of FAF adjacent to large, soft drusen and GA with the hyperpigmentation seen in AMD, several times greater than by chance. The investigators also noted that an increased FAF is not a major determinant of CNV, but is a sensitive marker for reticular pseudodrusen which, in turn, are associated with CNV.[75]

### THESIS PROPOSAL

To propose to outline a specific methodology: the Minnesota Grading System using fundus autofluorescence (MGS-FAF). This study will attempt to quantify FAF compounds in human eye bank donor tissue specimens in a standard manner and correlate these findings with the clinical finding from the MGS of AMD. Additionally, it will correlate the FAF changes with donor age in order to compare normal aging to pathologic aging. Finally, an internal fluorescence standard is proposed for use in future data collection.

In an editorial by Hopkins and coworkers,[72] a basic lack of standardization in FAF testing was discussed, specifically, variations in nomenclature, disease classification, and equipment used. The advantage of the MGS-FAF methodology over other studies is the added ability to correlate FAF to the clinical stages of AMD, based on the internationally accepted definitions of disease progression used in both the AREDS and BDES. In future studies, this association will enable us to correlate biochemical findings directly to the stages of clinical disease progression. Additionally, the MGS-FAF technique may be helpful with early-onset maculopathies that manifest autofluorescent compounds, such as Stargardt's or Best's disease.[51,63,80-82] Future biochemical discovery (beyond the scope of this thesis) will help us understand the influence of FAF in the early stages of the disease process.

In this study, the macular fundus is imaged using FAF ex vivo with the confocal scanning laser ophthalmoscope (cSLO; model HRA [first generation], Heidelberg Engineering Inc, Heidelberg, Germany).[79,82-84] The confocal terminology of the cSLO represents a combination of "conjugate" and "focal," meaning 2 sensors imaging the exact same plane of the tissue, therefore having a depth of field at approximately 300 μm, eliminating other "out-of-focus" tissue layers. This property allows for imaging a specific tissue plane, such as the RPE or neurosensory retina, and has numerous clinical and diagnostic advantages. In future studies, we hope to compare the findings of the MGS with those of the MGS-FAF to further define the biochemical and protein pathways that lead to progression of AMD.

## METHODS

### TISSUE PROCUREMENT

Donor eyes (262 eyes, 131 pairs) were procured for the Minnesota Lions Eye Bank. Ages ranged from 42 to 100 years with a mean age of 59 years. All tissue was acquired with consent of the donor or donor family. The consent is in accordance with the principles outlined in the Declaration of Helsinki. Investigators identified the eyes only by eye bank number to ensure confidentiality. Exemption status for this study was obtained from the internal review board at the University of Minnesota. For the majority of tissue collection during this study, eye bank procurement personnel selected globes by inquiring about a positive history of AMD with the next of kin. If an AMD history was reported, eyes were specifically transferred to our laboratory for analysis. Therefore, our study group was biased to select eyes that were more likely to have AMD. Globes were placed in moist chamber canisters at 4°C.

### DISSECTION

Globes were evaluated only if the time of death to analysis at our laboratory was 22 hours or less (mean, 10.7 hours). Eligible globes were processed immediately. Each globe was cut circumferentially at the pars plana to remove the anterior segment and provide a direct, unobstructed view of the macula. A 1000 ± 2.5-μm ruby sphere (Meller Optics, Inc, Providence, Rhode Island) was placed over the optic nerve to serve as a standard size reference. High-resolution, stereoscopic, color, digital fundus photographs (Sony DXC-S500, Japan) could then be taken through a dissecting microscope (Nikon SMZ-1500, Japan) of both the right and left macula and including the optic nerve. By rotating the globe and repeating the digital image capture, we were able to produce stereoscopic images.[16,21] Next, retinal tissue was carefully dissected and removed to expose the underlying RPE and choroid. The vitreous was removed as completely as possible with a Wescott scissor. The neurosensory retina was grasped with a 0.12-mm tissue forceps in the far periphery and gently peeled (along with the remaining vitreous) toward the optic nerve (analogous to pulling the sheets and covers off a bed). Scissors were used to excise the neurosensory retina from the optic nerve. Care was taken not to allow the tips of the scissors to touch the underlying RPE, and tissue manipulation in the macular region was avoided. If artifacts were created during dissection, these were noted and accounted for during grading. Artifacts were easy to detect as they were usually linear and outside of the central 6 mm of the macula. Instrument disruption artifacts were relatively common at the edge of the optic nerve and were useful during subsequent image analysis of FAF images.

### ILLUMINATION FOR DIGITAL, COLOR, STEREO PAIRS

Direct, tangential, and indirect (transscleral) illumination techniques were used to highlight drusen, pigment, and vascular structures. Direct illumination of the macula was obtained by using 2 flexible gooseneck fiberoptic cables, each attached to a halogen light source (Schott-Fostec, Auburn, New York). The illumination was oriented tangentially, along the side of the dissecting microscope. Indirect transillumination of the macula was obtained with a flat-mount, plate-style diffuse illumination system (Schott-Fostec, Auburn, New York).

### CONFOCAL SCANNING LASER OPHTHALMOSCOPE IMAGES

The images were obtained following standard techniques for digital, stereoscopic color images and globes were immediately transferred for cSLO imaging. On the basis of a series of 8 globes tested over the first 2 hours and 20 minutes of machine operation time, the machine was warmed up for at least 1 hour in advance of the image acquisition (Figure 1). The sensitivity setting (detector gain control) on the cSLO control panel was preset at a precise, predetermined setting and remained identical for each eye studied.

The globes were imaged with a ruby sphere placed on or near the optic nerve with a 20 diopter, double aspheric lens between the cSLO and the donor eye. This enabled a proportional image in the setting of an open globe, without anterior segment structures (eg, a cornea and lens). Note that the neurosensory retina was removed as part of the MGS grading stage and is therefore not present on any of the FAF images. Using several trial globes, eyes were imaged repeatedly between 10 and 22 hours postmortem. There were no significant changes in the FAF of these globes during this brief interval.

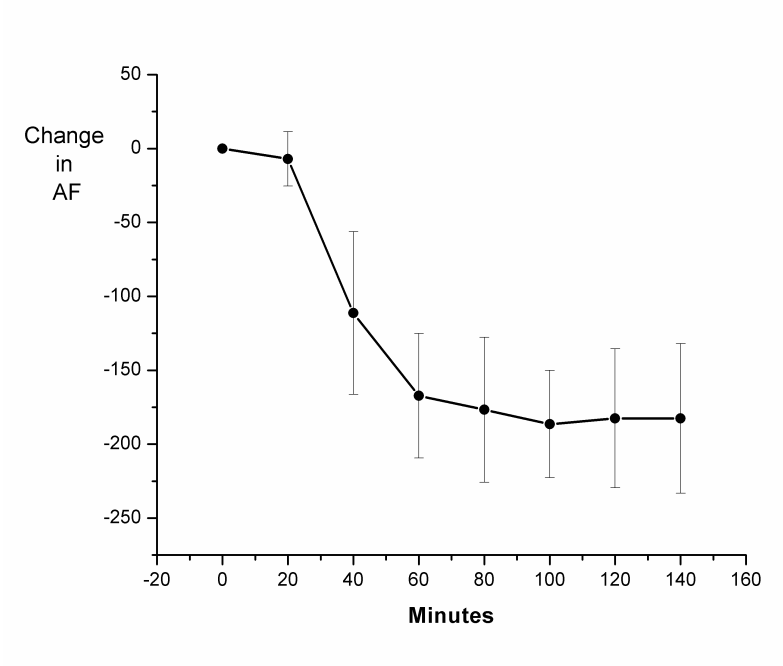


**FIGURE 1**

Standardization curve for fundus autofluorescence (AF) vs time. The AF of the confocal scanning laser ophthalmoscope (cSLO) is compared to 140 minutes time from start-up. The data points (± standard deviation) were based on standard change in mean AF image intensity from baseline, taken on the same globes at the specified time intervals. Note how the AF intensity is extremely high at the initial start-up of the cSLO and slowly decreases over time. By 1 hour, the curve flattens and the subsequent measurements become more reproducible. The AF scale is in arbitrary units and represents the change in fluorescence density; therefore, numbers are negative when the images become less fluorescent.

Next, the globe was suspended for direct imaging with the cSLO using the infrared setting, and the FAF mode with the argon excitation light at 488 nm, and the detection spectrum with a long-pass filter >500 nm. Eyes that did not have any peripapillary pigment irregularities had a small intentional artifact created. This mark allowed for proper orientation of the FAF images and comparison to the digital color overlay images as described below. The standardization curve was important in order to determine the time required for reproducible cSLO image acquisition. The resultant images (Figure 2) demonstrate the importance of adequate warm-up time when using this technology, especially with dependence on grayscale analysis of FAF images. This technical variable is not specifically referred to in other publications of cSLO image analysis. Therefore, we assume that this variable has not been adequately controlled or accounted for in current clinical studies and analysis of FAF using the cSLO. The property of FAF means that a material, such as LF, will absorb a certain wavelength ($\lambda$) of light and emit a longer wavelength that will be detected by specific sensors. The cSLO illuminates the retina with narrow bandwidth blue laser light energy ($\lambda$ = 488 nm). The major fluorophore in the ocular fundus is the LF material.[83] The LF, within the RPE, absorbs the blue light level of energy and emits a longer-wavelength green light with a peak emission between 550 and 600 nm.[85] A "long-pass" barrier filter is placed between the detector and the fundus in order to block reflected light ($\lambda$ < 500 nm) but detect the longer-wavelength green light. The monochromatic laser excitation at 488 nm combined with a 500-nm barrier filter and confocal detectors localize the tissue and create a very specific and efficient mechanism for detecting FAF at the RPE. In the future, with improvements in technology, dual illuminators or detectors could be incorporated.[86]

## IMAGE ANALYSIS

Digital images from the cSLO machine were imported into the image software program (Adobe Photoshop CS, version 8, San Jose, California) for grayscale pixel analysis. First, the digital color fundus image was layered over the FAF image for size and orientation analysis (digital, stereoscopic color images used to analyze the tissue in accordance with the MGS[16]). The color and FAF images were opened in either red-green-blue (RGB) or grayscale mode, respectively. Grayscale and color images can be compared directly because the luminosity of the images is comparable. The image was scaled to size and arranged so that the color fundus image landmarks of the optic nerve were positioned over the optic nerve landmark in the FAF image. Both the ruby sphere and the peripapillary artifact allowed for exact size and orientation, rotational alignment, and agreement between the 2 images. The size is confirmed in exact measurements using the 1000-µm ruby sphere as outlined in the MGS.[16] In the layers menu, the opacity was changed so both images were viewed at the same time. Figure 3 represents transitional overlay images of the color to FAF image. The size and orientation of the grading rings are based on the precise size reference from the MGS color image with the associated standard ruby sphere (1000 µm). The peripapillary artifact allows for exact orientation of the grid to match the foveal orientation. Combining the peripapillary artifact and the foveal reference point (generated using techniques of the MGS), precise FAF macular localization and orientation for the grading template are ensured. The center ring is exactly 1000 µm, and the inner ring is proportionally matched to the center and

outer rings (3000 and 6000 μm, respectively). These rings allow for a reproducible and reliable size reference, directly at the macula. Moreover, the sizes correspond to the size references in the MGS, AREDS, and BDES (based originally on the Early Treatment of Diabetic Retinopathy Study [ETDRS] template).

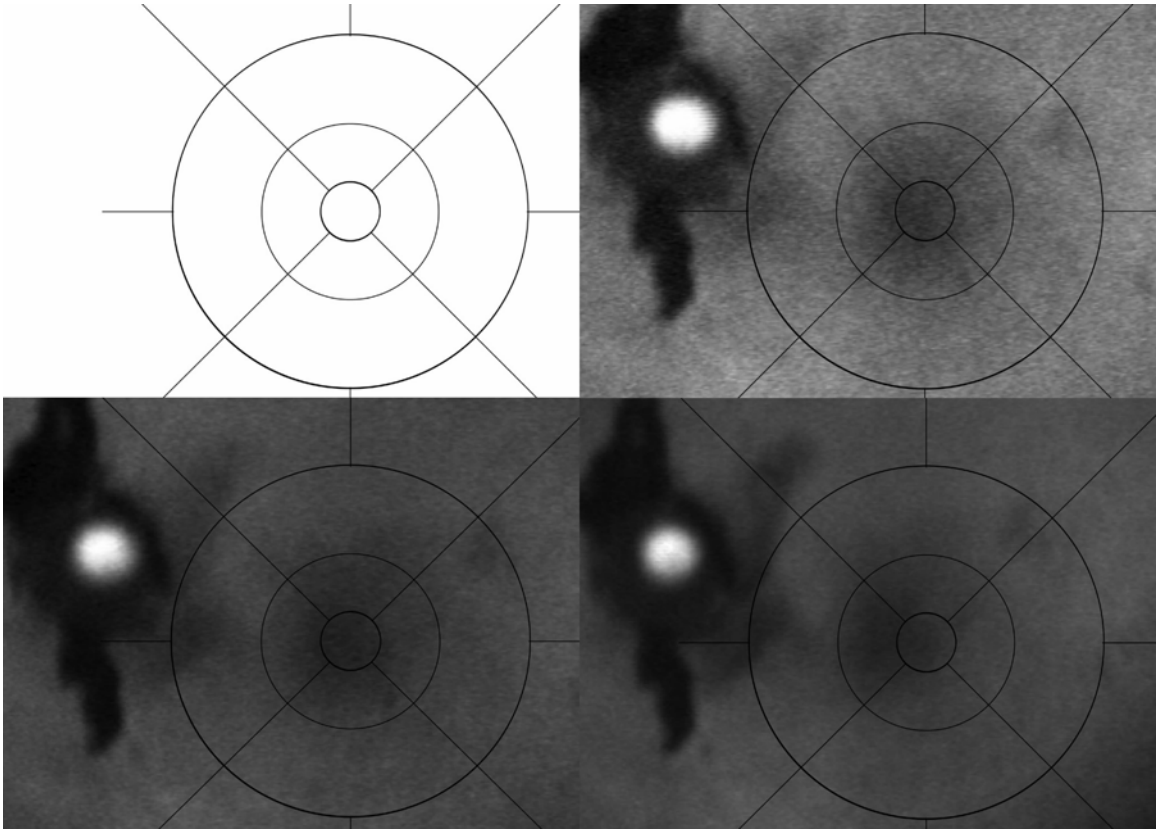

**FIGURE 2**

Fundus autofluorescence (FAF) images taken at various times within the first hour after start-up of the confocal scanning laser ophthalmoscope (cSLO), demonstrating the changes in "apparent" FAF over time on the same specimen. Upper left, Image taken upon start-up shows a bright white washout that makes analysis impossible. Upper right, Image taken at 20 minutes demonstrates a bright but discernable FAF image of the left macular region. The grading template (dark circular lines) and the ruby sphere (bright white circle) are easily visible. Lower left, Image of the same globe taken at 40 minutes with less "apparent" FAF. Lower right, Image taken at approximately 1 hour shows no change in "apparent" FAF at later times.

Next, the FAF image data acquired with the grid were analyzed using the histogram grayscale setting on the Photoshop CS software program. The results are displayed with pixel luminosity ranging from 0 to 255 (arbitrary luminance density units). We selected a low-end cutoff of <38 units and a high-end cutoff of >250 units. This was automated so that any units outside of this range were eliminated from analysis. The purpose was to exclude areas of GA as well as bright, artifact-related light reflexes from interfering with true FAF intensity measurements. The mean FAF over the graded templates could then be analyzed by multiplying the luminosity readings (38 to 250 units) within the designated region of the grid by the number of pixels and dividing this by the total area to give a measure of total FAF (tFAF):

$$\text{tFAF} = (\text{luminosity} \times \text{pixels})/\text{Area}$$

This formula subtracts out the areas of artifact automatically by removing both the luminosity scores <38 or >250 and the accompanying surface area of the eliminated pixels. Therefore, the tFAF measurement represents an accurate analysis of mean FAF within the macular region, given the in vitro testing circumstances. Figure 4 demonstrates an FAF image with GA and bright white light reflexes. The automated cutoff generated by the software program eliminates both the dark areas of GA and the bright white reflexes and analyzes the resulting FAF for luminosity using the histogram. Numerical values for tFAF may be generated for any desired region: center (C), inner (I), outer (O), or any combination of rings. Some large choroidal vessels within areas of GA may fluoresce. This represents a potential source of error in analysis of eyes with GA. The center ring encompasses the center 1000 μm, the inner ranges from 1000 to 3000 μm, and the outer ring extends from 3000 to 6000 μm.

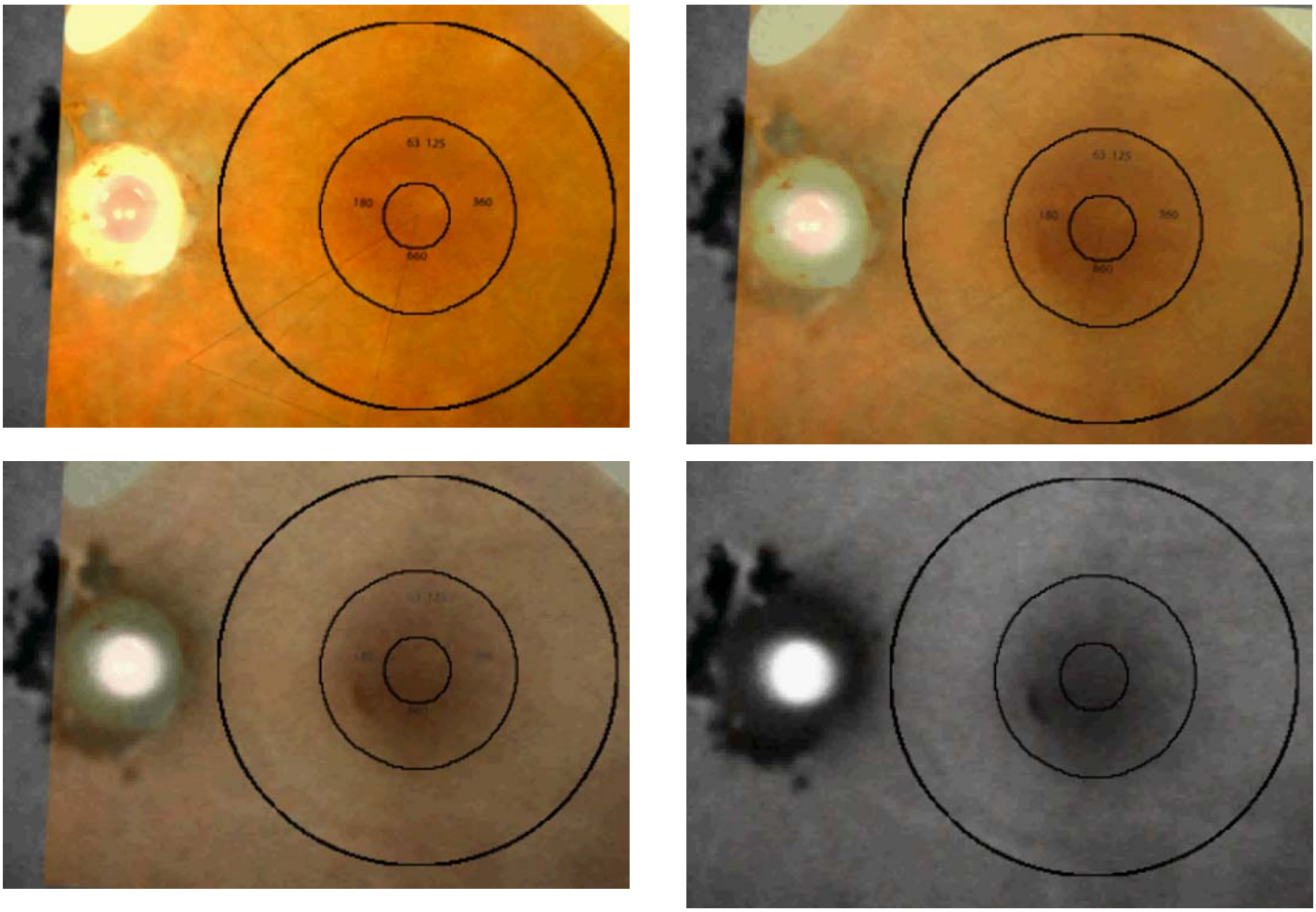

**FIGURE 3**

Digital color and fundus autofluorescence (FAF) image overlays, demonstrating the transitional overlay of the color fundus image to the FAF image that ensures accurate size and orientation analysis (especially relative to the macula). Upper left, Color image is dominant over the FAF image and has peripapillary irregularities (outside of the grading circle) and a visible ruby sphere on the optic nerve. Upper right, Gradual fading of the color image, with a more prominent view of the FAF image and the dark black–appearing peripapillary artifact. The ruby sphere is easily recognized for size reference (matches the 1000-µm center ring of the macular grading template). Bottom left, Faded color image over the dominant FAF image is seen, as well as the correspondence of the macular region and the peripapillary artifact for orientation. Bottom right, Removal of the color image, with the grading rings oriented properly for size and centered directly on the macula.

## INTERNAL LUMINANCE REFERENCE BEAD

After acquiring the images from eye bank tissue for this work, and analyzing the data, we theorized that adding a luminance reference bead on our FAF images would allow for an internal luminance intensity control reference. We used a series of colored beads or color strips with autofluorescent properties. For each of these materials, we performed a warm-up phase analysis (Figure 5) on each color of bead: Alexa Fluor 488, a ruler strip, green bead, sapphire bead, orange strip, yellow bead, magenta bead, and a turquoise bead. The luminance dropped from a peak upon start-up of the cSLO, to a stable level after 1 hour. This corresponds to the warm-up time that we determined from the FAF readings of the human tissue (Figure 1). Figure 5 shows an example curve for a turquoise color of autofluorescent bead compared to Alexa Fluor 488. The turquoise bead luminance measurement stabilizes at a baseline luminance level with only minor variability. The goal was to identify a reference bead that would stabilize as near as possible to a midpoint of eye bank FAF tissue. The turquoise color bead seems optimal.

Therefore, by calculating an adjusted tFAF (atFAF) that compares the difference of the cSLO reading from the pixel luminosity density at each pixel

$$\text{atFAF} = (\text{tissue} - \text{reference luminosity})/\text{Area}$$

Results of the atFAF would therefore represent the mean FAF of a given area relative to the fluorescent control. If there is less FAF than the mean FAF of the reference bead, the value may be negative. For example, if the mean tissue FAF of a given area is 85, but the reference bead is 100, the taFAF would be −15. On the other hand, if the mean tissue FAF of a given area were above 100, the taFAF would be a positive number. Further mathematical modeling is possible. Smith and coworkers[75] have described the mathematical modeling of focal increased or focal decreased FAF as they relate to drusen and other fundus features. Similar modeling and comparison to color images of drusen and pigment irregularities is possible using the methodology described herein. For example, correlating drusen type, GA, focal areas of hyperpigmentation, and reticular pseudodrusen is possible using the modeling described.[75] The advantage of this system is the ex vivo status, allowing for future studies investigating histopathology or biochemistry.

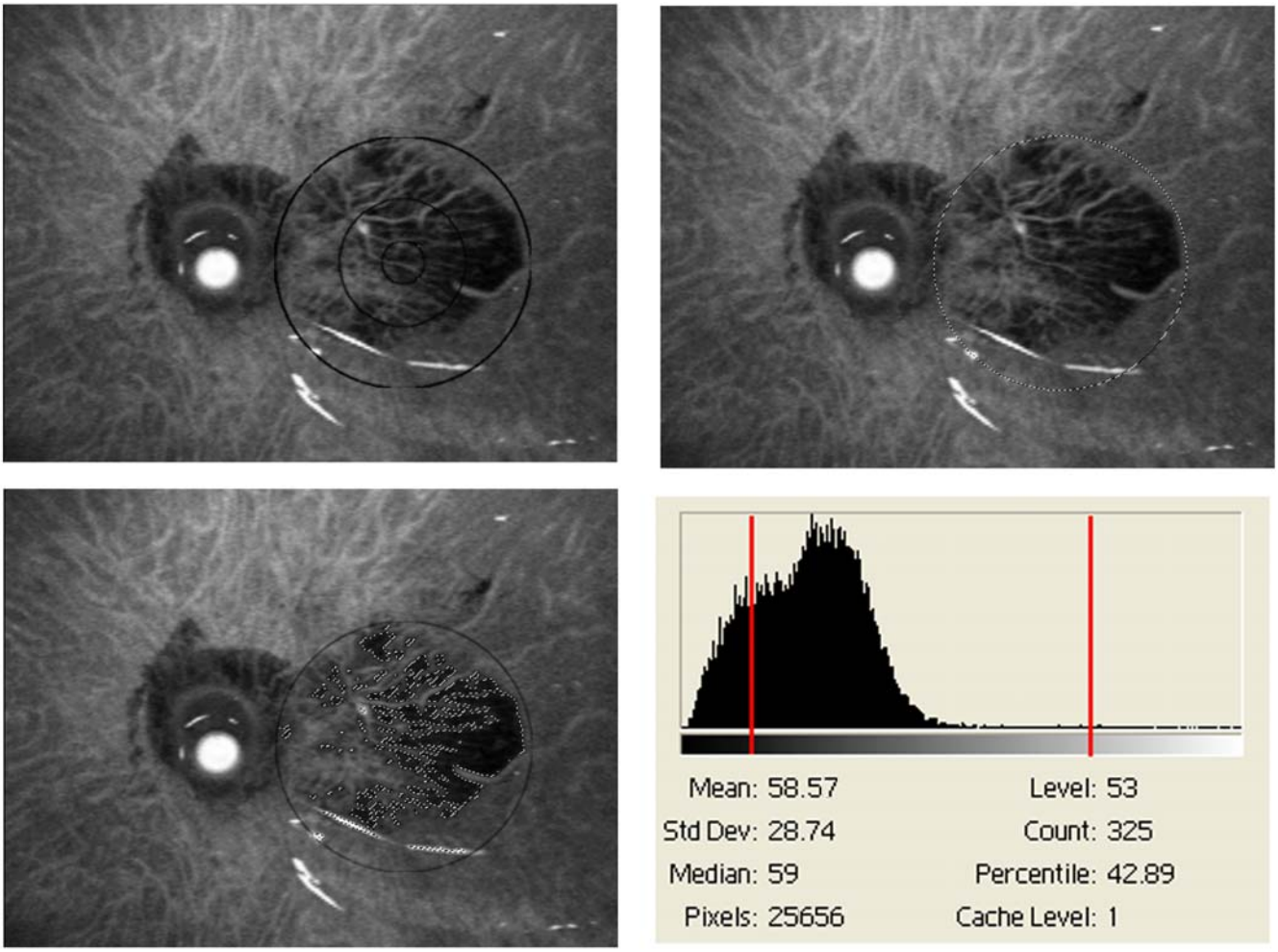


**FIGURE 4**

Digital image representation used to calculate mean autofluorescence. Three images and a histogram demonstrate the computerized analysis of the FAF image using a program that eliminates dark areas of geographic atrophy (GA) and artifactual white light reflexes from analysis. Upper left, FAF image of an eye with advanced age-related macular degeneration represented by central GA (dark area). Upper right, Computer-generated circumference ring of 6000 μm, generated in reference to the grading template. Bottom right, Resultant histogram shows the luminosity units over the pixel range. Bottom left, Zones removed by the computer analysis to eliminate zones of GA and light reflex, shown numerically as red vertical lines on the histogram (elimination of luminosity <38 or >250). The MGS-FAF scale is in arbitrary fluorescence density units.

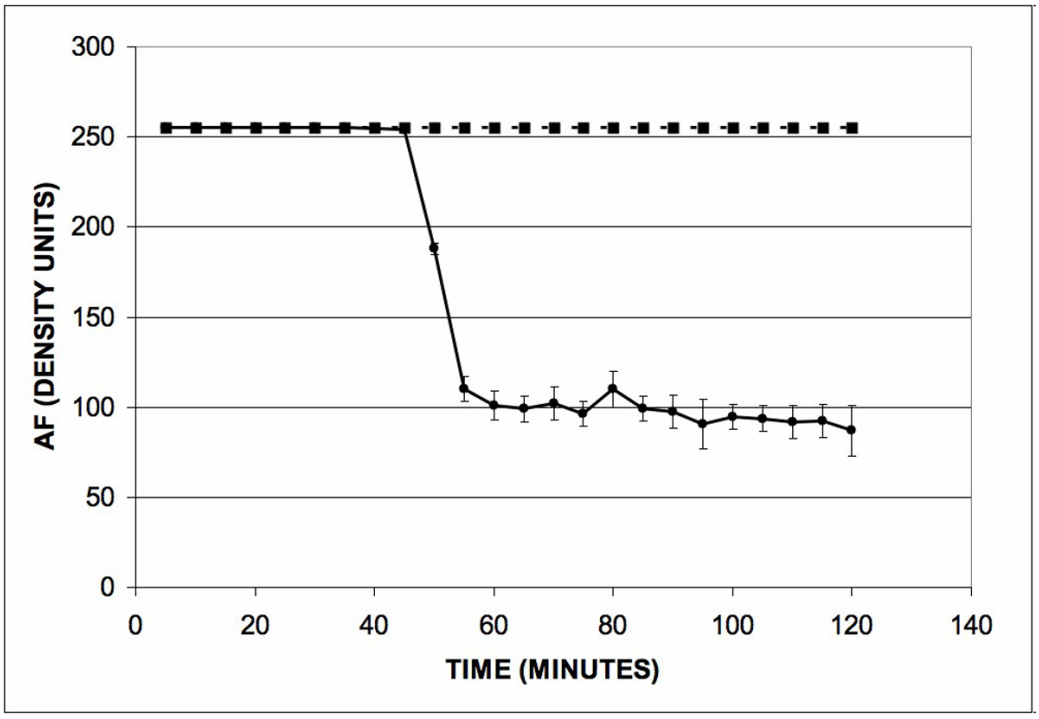


**FIGURE 5**

Standardization curve for fundus autofluorescence (AF) of the confocal scanning laser ophthalmoscope over 120 minutes from start-up. The data points (± standard deviation) were based on standard change in mean AF images intensity from baseline. A standard, highly fluorescent material was used for comparison (closed box) and is represented by the line that remains constant at 255 density units. A turquoise bead is used (closed circle) that has a stable AF after 1 hour at approximately 100 density units. Multiple fluorophores were tested, but the turquoise was the most stable fluorophore in the desired range.

## RESULTS

### THE MGS AND AGE

The first objective is to carefully analyze the relationship between the MGS and age to confirm the known association that more advanced cases of AMD as graded by the MGS (using an in vitro system of AMD analysis) correspond to increasing age. Indeed, Figure 6 demonstrates quite convincingly that there is a strong association between MGS level (1 through 4) and increasing age. There are noted "outliers" in the data. Specifically, there is an MGS level 4 at age 42 that represents a traumatic maculopathy, rather than AMD. In reviewing this pair of globes, the fellow eye was normal, graded as MGS level 1. Eliminating this data point would not change the strong association of MGS and age. Overall, this evidence supports existing evidence that age is a major and significant risk factor for AMD.

### MGS-FAF AND AGE

Many studies acknowledge that there is an increase in the LF pigments with increasing age.[48-50] The digital subtraction methodology (namely, the elimination of areas of GA or RPE cell loss) was used to address this issue in a standardized manner. Using the MGS-FAF, we looked at the association of LF to age by comparing the center (C), inner (I), outer (O), and a combination of all areas (C+I+O) in 263 eyes with age and found no statistically significant association of LF and age (Figure 7). The lack of association of age and FAF, despite looking at all macular regions, is very interesting. This suggests that the MGS-FAF system does not detect either an increase or a decrease in LF in the 42- to 100-year-old population of eye bank eyes. By subtracting areas of GA or artifact (<38 or >250), we are not able to show that FAF increases in any statistically significant manner. Breaking down the regions of the macula into specific subfields (center, inner, outer, or any combination), we tried to identify regions that may be more susceptible to increasing or decreasing LF deposition. The regions imaged were areas that were not excluded by the software analysis. Therefore, this analysis likely represents areas of viable RPE. This model allows for a view of the RPE only, without the influence of the luteal pigment of the neurosensory tissue (removed). Therefore, the decreased relative FAF in the foveal center is likely mostly accounted for by the increased pigmentation (taller and more columnar cells) of the subfoveal RPE, partially masking the FAF. Alternatively, there is simply less FAF or LF in the healthier central RPE than in the surrounding RPE. Finally, our statistical analysis treated each eye independently, yet each had a paired globe. Considering these eyes independently would pose some limits on statistical analysis.

Regardless, there are individuals with differing AMD levels in one eye vs the fellow eye. The large number of globes or pairs included should help minimize this potential bias.

**MGS-FAF AND AMD**

The association of FAF and AMD is variable in the literature. There is not a clear association of FAF, presumably a measure of LF and AMD. Figure 8 demonstrates that there is a clear association of MGS-FAF with AMD as graded using the MGS 1 through 4. Statistical analysis using the Tukey-Kramer analysis shows a significant difference in MGS-FAF from MGS level 1 or 2 to MGS level 3 or 4 ($P < .0001$). Polynomial linear analysis also indicates this level of significance. The MGS-FAF is also significantly decreased from MGS 3 to MGS 4 ($P < .0001$). This provides rather strong evidence of an association of LF in the early stages of AMD, with a decline in the later stages of AMD. This is particularly relevant because we did not show any trend or association of MGS-FAF with age (Figure 7). These data indicate that there is a loss of fundus FAF in more advanced stages of AMD, particularly when the clinical phenotype suggests a higher risk. Eyes at level 3 or 4 demonstrated a benefit from taking antioxidant supplements with zinc, compared to no benefit in those at level 1 and 2 in the AREDS. The loss of MGS-FAF suggests that there is a decline in the total amount of FAF outside of artifact zones (such as areas of GA). An association of focally increased areas of FAF has been noted in AMD, especially at the edges of soft drusen or geographic atrohy.[75,87-89] Again, clear reports of generalized levels of FAF in prospective studies are lacking. There are variable findings using differing FAF imaging techniques with no clear determination of an association between mean FAF and progressive AMD.[75,76] We attribute much of these discrepancies to a varied, nonstandardized method of analysis using differing technology. Standardization is required to properly answer this question, as suggested by Hopkins and coworkers.[72] While focal areas of increased FAF may be associated with higher-risk AMD, a mean level of FAF, as defined by the MGS-FAF, with precise definitions of AMD and a reproducible methodology, demonstrates a statistically significant decreased level of mean FAF in progressive stages of AMD.

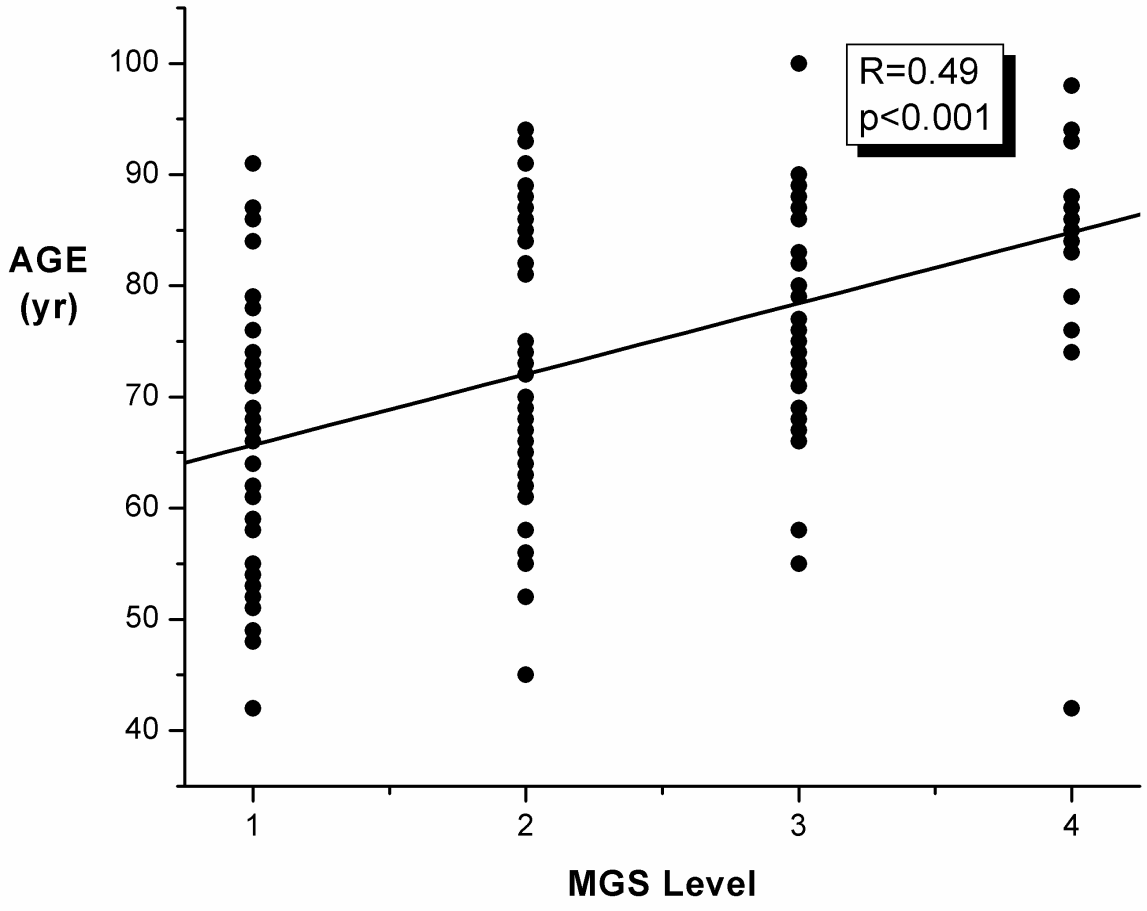


**FIGURE 6**

Scattergram of age (in years) vs MGS levels 1 through 4 in 262 donor eyes graded according to the MGS system[16] shows a strong positive correlation between MGS severity (more advanced age-related macular degeneration) and increasing age ($R = 0.49$, $P < .001$).

## MGS-FAF AND CLINICAL IMAGES

The clinical appearance of various macular pathologies was highlighted using the combination of the MGS and the MGS-FAF. For example, the details of basal laminar drusen (also called cuticular drusen) are well documented in the MGS. Drusen are hypofluorescent in the MGS-FAF (Figure 9). Recently, reticular pseudodrusen have been noted to hyperfluorescence clinically.[75] Reticular pseudodrusen are a relatively less common clinical feature seen in cases of AMD and are represented in Figure 10, using both the MGS and MGS-FAF. Our imaging technology demonstrates an excellent ability to detect and diagnose other clinical features of AMD, despite the fact that our tissue imaging is done postmortem.

Interestingly, 95 of the 262 eyes examined (36%) had a "ghost image" of the retinal vessels that were seen as hyperfluorescent on FAF imaging. The exact cause of this pattern of hyperfluorescence is unclear, especially when the neurosensory retina and the retinal vasculature were removed prior to the FAF imaging. A direct, side-to-side comparison of the retinal vasculature to the hyperfluorescent "ghost image" confirms that the pattern is from the retinal vessels (Figure 11). We speculate that the blood within the retinal vasculature may shield the underlying fluorophores from the photographic white light imaging done prior to dissection of the neurosensory retina. Alternatively, there may be biochemical factors present within the blood vessels that alter the underlying RPE, resulting in increased FAF. Perhaps an effect on the pigment within the RPE could unmask fluorophores.

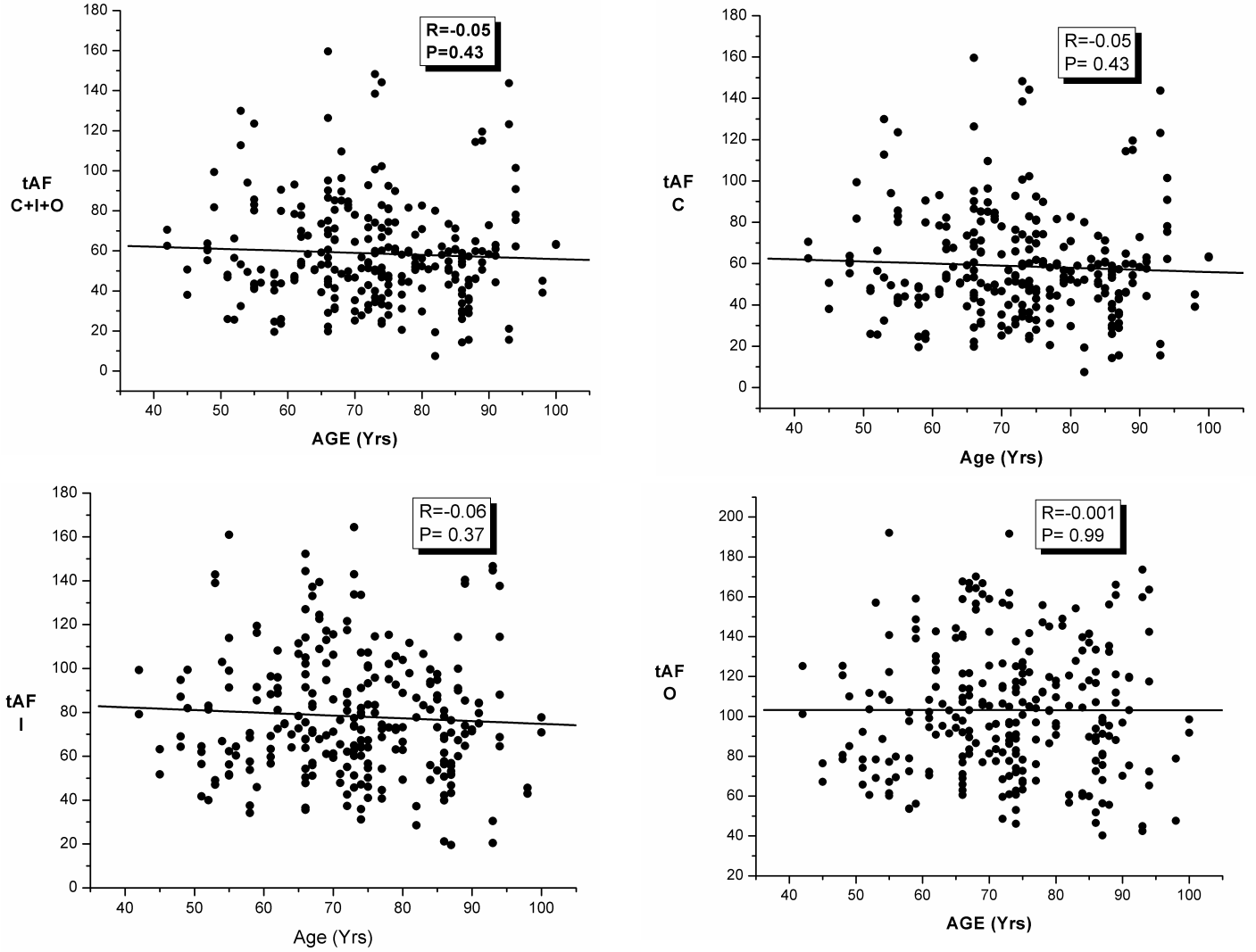


**FIGURE 7**

Scattergrams comparing the MGS-FAF with age using various regions of the macula comparing mean fluorescence density units (y-axis) to age in years (x-axis): Center (C), inner (I), outer (O). Upper left, MGS-FAF regions C+I+O compared to age, with no significant association ($P$ = .43). Upper right, MGS-FAF in region C compared to age, with no association ($P$ = .43). Lower left, MGS-FAF in the inner region (1000 to 3000 μm) compared to age, with no association ($P$ = .37). Lower right, Outer MGS-FAF in the outer region (3000-6000 μm), with no association ($P$ = .99).

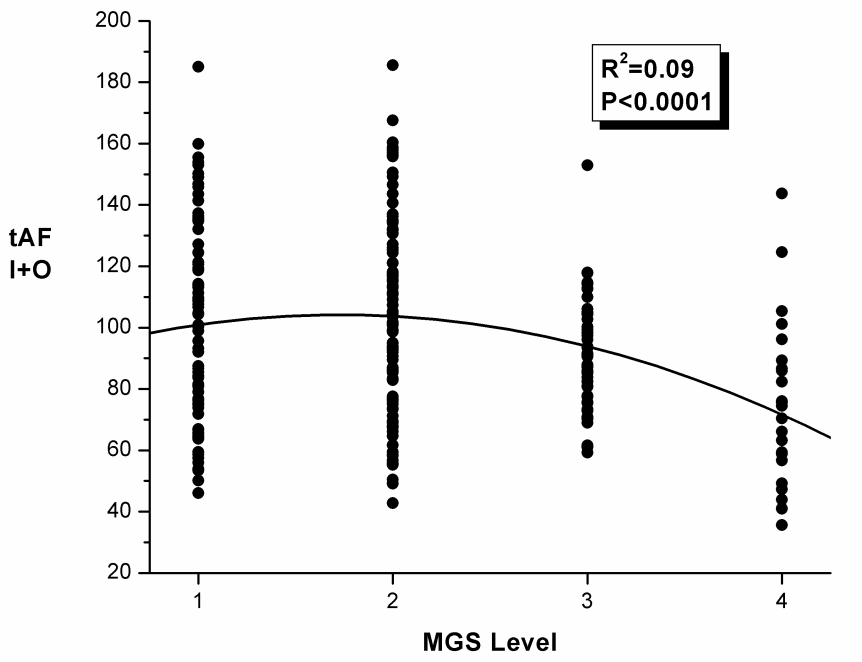


**FIGURE 8**

Scattergram comparing total fundus autofluorescence (tFAF) in mean fluorescence density units to the MGS level of age-related macular degeneration. The peak in the tFAF units occurs at MGS level 2 ($P$ = .002; Tukey Kramer analysis) and declines significantly at MGS level 3 ($P$ < .001) and MGS level 4 ($P$ < .001). Using polynomial regression analysis, this trend is significant ($P$ < .001).

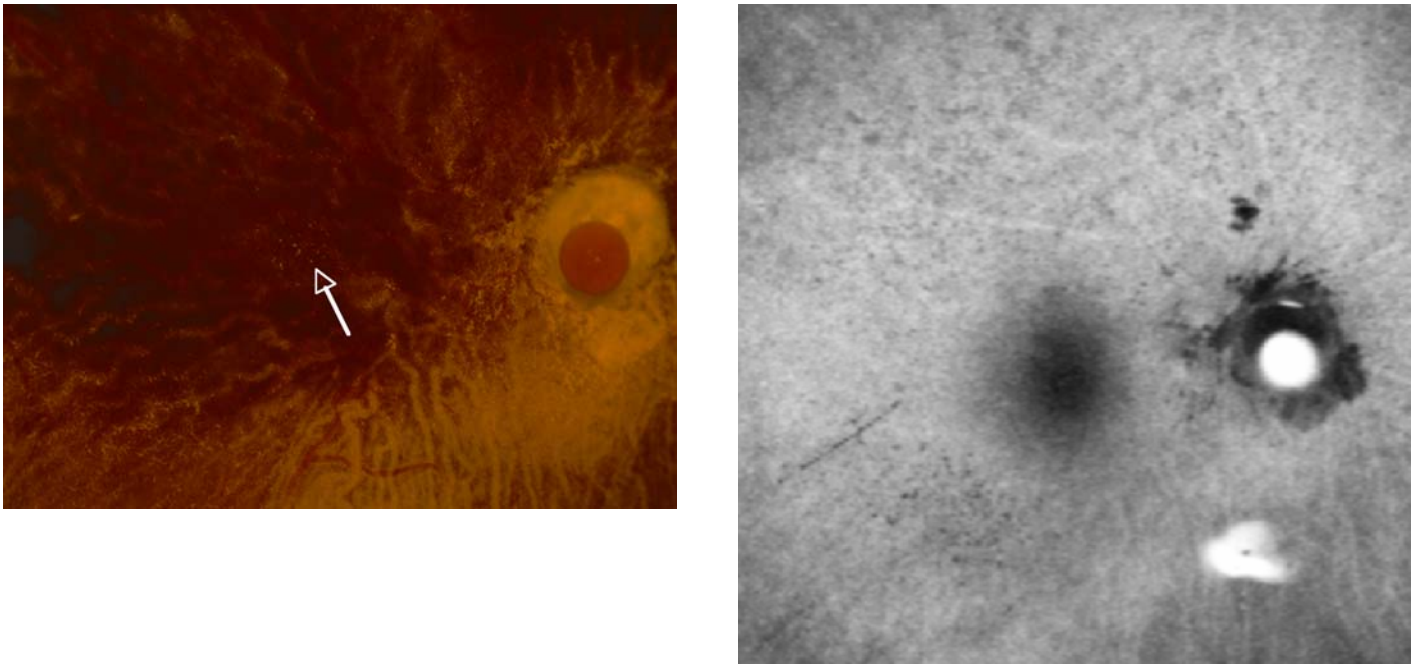

**FIGURE 9**

Basal laminar drusen or cuticular drusen are easily seen in the color photograph as small yellow dots (<100 µm) in the macular and peripapillary region (left). Comparing directly to the fundus autofluorescence (FAF) image (right), the drusen correspond to areas of hypofluorescence. Note that the surrounding area in the FAF image is rather bright (hyperfluorescent), suggesting the presence of lipofuscin (LF) in this 89-year-old woman graded with MGS level 2 age-related macular degeneration.

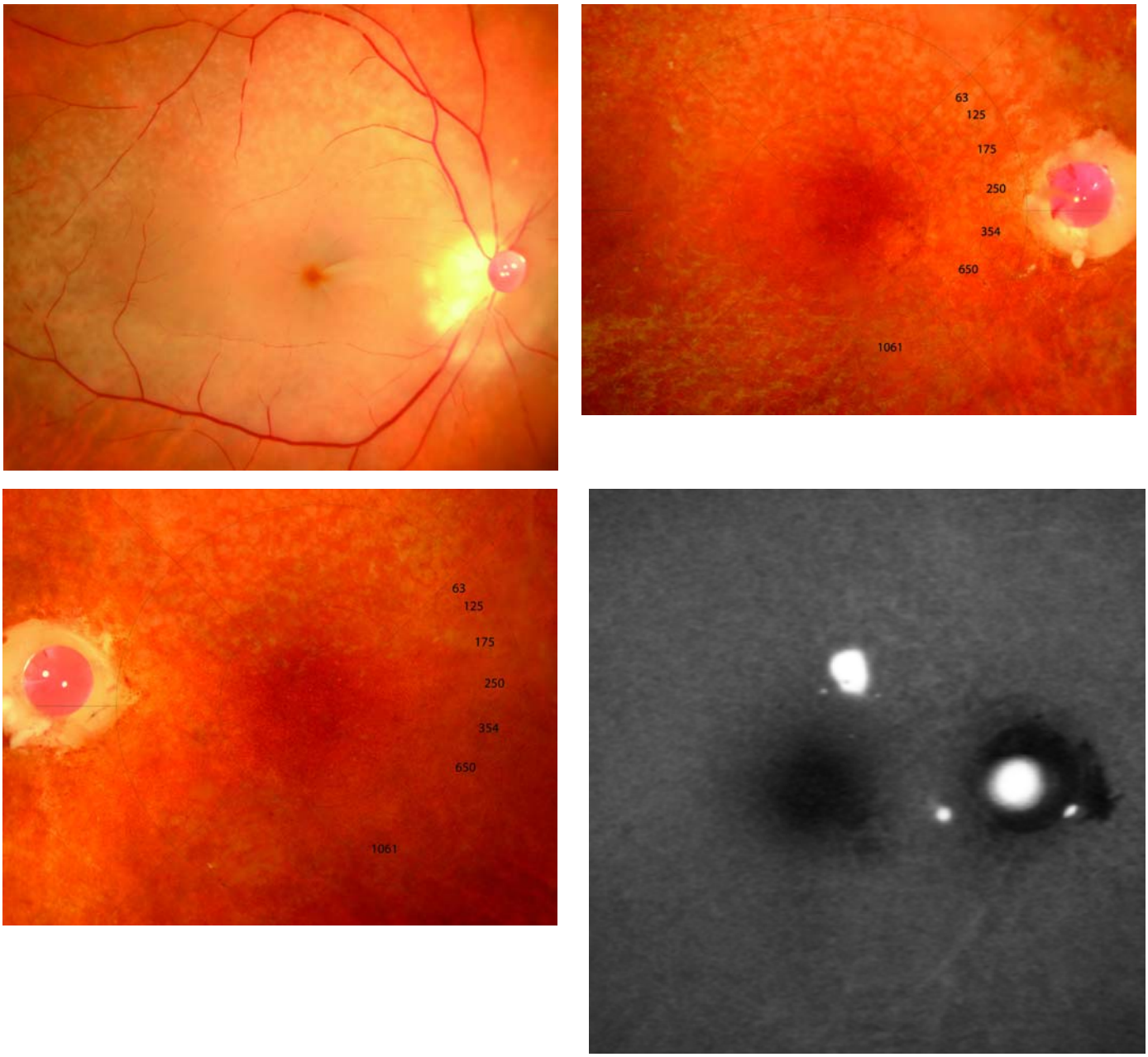


**FIGURE 10**

Photographic demonstration of reticular pseudodrusen, an uncommon clinical finding that is represented using both the color and fundus autofluorescence (FAF) image. Upper left, First photograph taken in the MGS series, of the partially opaque neurosensory retina in an eye with reticular pseudodrusen, best seen in the superior temporal quadrant as a reticular (netlike) pattern of yellow material. The neurosensory retina is removed and both the right (upper right) and left (lower left) demonstrate both typical drusen near the macula (center ring) and reticular pseudodrusen, best seen in the superior outer ring of the grid in either eye. The FAF image (bottom right) shows the hyperfluorescence of the reticular pseudodrusen in a similar pattern that corresponds to the color image (note the artifact light reflex that is bright white). Numbers on the grid represent the diameter (in μm) of the circle.

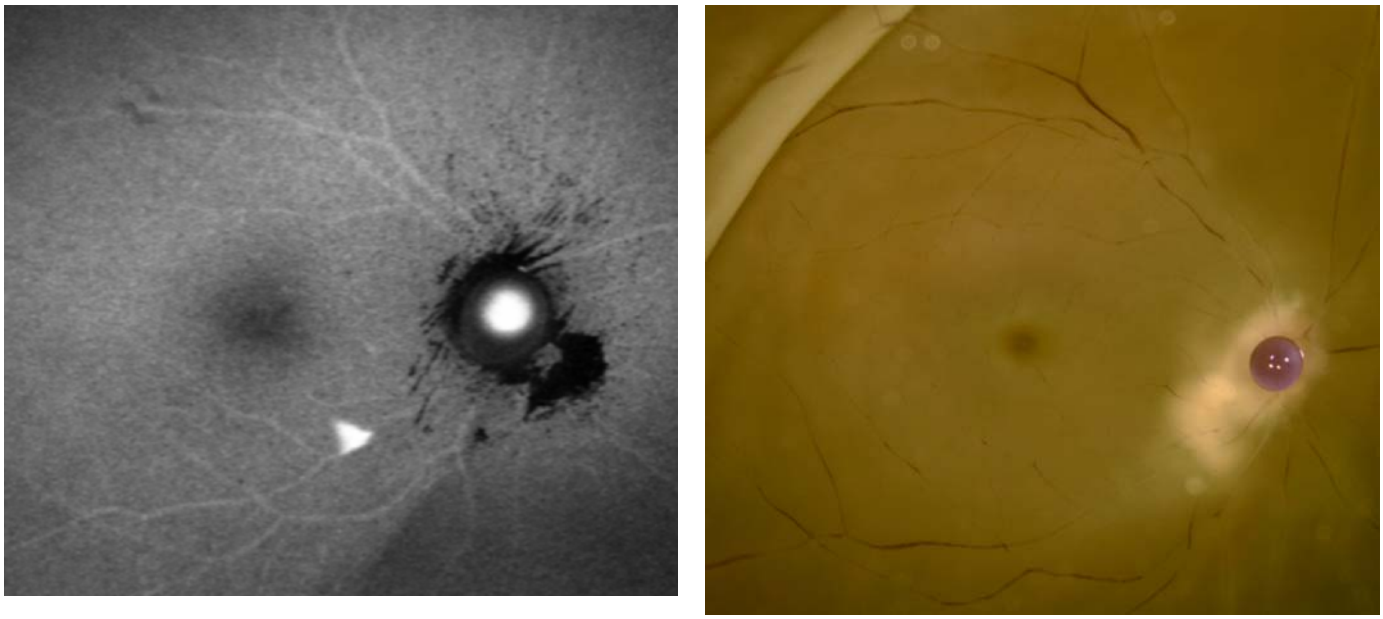

**FIGURE 11**

Digital image of "ghost vessels." A comparison of the fundus autofluorescence (FAF) image (left) that corresponds to the retinal vasculature (right), which remains in the FAF image, even after the retinal vasculature has been removed. Note that the image on the left has already had the neurosensory retina removed, so the retinal blood vessels are not actually present. This "ghost image" phenomenon was common (95 of 262 cases [36%]).

### INTERNAL LUMINANCE REFERENCE BEAD

The fluorescent beads or strips of varying color offer a variety of baseline FAF intensities that could be used as a future internal fluorescent standard control. By comparing the mean FAF to a standard luminance reference, calculations could be further standardized and less dependent on the stability of the laser illumination, the detectors, or sensors. While any of the beads may be used, the bead that is closest to the midpoint of our intensity data is the turquoise bead with an FAF luminance near 100 units. The less fluorescent sapphire bead has a lower standard deviation and may be useful, especially with a comparison to tissue that has low tFAF luminance levels. While none of the tissue analyses presented in this study were obtained using the FAF reference bead, the inclusion of these data in future analysis will help to optimize and standardize this methodology.

## DISCUSSION

Our understanding of the aging process continues to evolve. A rationale, scientific approach to studying normal vs pathologic aging will help us to understand basic mechanisms in age-related disorders. Hopefully, we will be able to identify changes occurring early in the disease process, allowing more time for effective therapy or lifestyle modification. In some individuals, aging occurs without development of disease. In others, pathologic aging results in a progressive degenerative state that becomes manifest as advanced AMD.

In the eye, LF has frequently been associated with both metabolic function and aging by multiple investigators.[48-51,54,85,90-95] In postmitotic cells, such as the RPE, LF accumulation from the primary fluorophore A2-E (N-retinylidene-N-retinylethanolamine) leads to incomplete lysosomal degradation, loss of membrane integrity, and increased phototoxicity.[63] Accumulation of this LF material leads to what has been referred to by some as a "garbage catastrophe" and is particularly challenging to prevent or treat.[96]

Using the MGS-FAF, we are able to detect and accurately quantify LF in the RPE using FAF techniques in a standardized and reproducible manner. Moreover, we are able to carefully document and compare the FAF findings to the clinical classification of AMD used by the AREDS through common, internationally accepted clinical definitions. We have adapted a grading template from the AREDS that has a precise size reference to accurately assess surface area.

This study documents a strong and statistically significant correlation of MGS-FAF and stage of AMD, based on direct comparison of the MGS to the MGS-FAF using both polynomial analysis (Figure 8; $P < .0001$) and the Tukey-Kramer, multiple comparison test. (This test is used when all pairwise comparisons of the means are tested. The test is not exact but is conservative for unbalanced 1-way ANOVA.) The MGS level 1 vs 2 has no significant difference, yet MGS 1 and 2 each have a higher mean FAF than MGS 3. Likewise, MGS levels 1 through 3 all have a significantly higher mean FAF value than MGS 4. This is a significant difference, with higher levels of FAF in MGS levels 1 and 2 and declining in the later stages of the disease. Results suggest that LF is

present in higher quantities in earlier stages and may play a role in the initiation of cellular events occurring in early stages of AMD. Loss of RPE, along with the accompanying LF contained intracellularly, in the later stages may account for a decreasing mean MGS-FAF level at the end stages of the disease. Apoptosis of the RPE from the aging process may be responsible for this decline. While there is significant clinical evidence that FAF increases focally around areas of high-risk clinical features,[75] measures of mean FAF decline in the later stages. Focal areas of increased FAF may result from unmasking of FAF at borders of RPE loss, possibly as a primary finding, but may represent a secondary finding in advancing stages of AMD. Diffuse irregularity of FAF in a region of the macula with AMD usually increases the risk of progression.[75,88] Similarly, focal areas of hyperfluorescence around pigment irregularities may also represent areas of melanolipofuscin, a form of complex granule that does not seem to occur as a direct result of photoreceptor outer segment turnover.[48,97-100]

In this analysis, we did not demonstrate a significant correlation of mean FAF levels to increasing age. A positive correlation in mean MGS-FAF was expected with increasing age, especially in the relatively large sample size (262 eyes). However, with MGS-FAF of the entire macula (6 mm), or any combination of macular region (center, inner, or outer), we found no relationship between MGS-FAF and age (Figure 7). There are several possible explanations for this finding. First, subjects' ages ranged from 42 to 100, but were mostly older than 50. Interestingly, the sharpest increases in LF have been reported in the first or second decades.[93] This raises an important question. When does the aging process actually begin? This question remains unanswered and is currently debated among researchers who study aging. A selection bias for eyes with AMD is included in the screening process by the eye bank procurement staff. Death rates of young individuals are low; thus we do not have adequate tissue to address this question from the eye bank population at this time. Therefore, we clearly have a bias toward middle-aged to older individuals in our series. Another plausible explanation would be that although LF is increasing in each individual RPE cell, the increase is offset by a loss of overall RPE cell number with increasing age.

Other investigators have seen similar lack of correlation with age in vivo.[101] Wing and colleagues[95] report a lack of correlation of LF content ratio (posterior pole/total RPE) when plotted as a function of age. They speculate that cellular dysfunction and death occur to account for this lack of correlation. However, they describe a significant increased *total* LF content, when plotted against age. As mentioned, other investigators have concentrated on the pattern of fluorescence and suggested that focally increased FAF is associated with reticular pseudodrusen, GA, pigment abnormalities, and large drusen.[75] The hyperfluorescence seen in Figure 10 supports the association with reticular pseudodrusen, whereas smaller drusen (such as basal laminar drusen) remain hypofluorescent (Figure 9). The MGS-FAF allows us to detect these altered clinical phenotypes and may be useful in the future for analysis of the acquired tissues with these more atypical phenotypes. Separation of various clinical entities may eventually lead to unique findings at the biochemical, proteomic, or possibly the genomic level through either gene expression analysis, microarray, or serial analysis of gene expression (SAGE).[102]

Proteins represent the building blocks of our cells. Understanding the proteome or basic cellular profile of a given tissue, such as the RPE or neurosensory retina, will improve our ability to understand biochemical events occurring at the cellular level.[17-23] While genes guide the cellular events, aging plays a role in the function and structure of the proteins and lipid membranes through oxidative mechanisms and abnormal protein folding. These events may lead to a proteotoxic state and early loss of cellular function.[103] The formation of abnormal intracellular and extracellular deposits that occur with time can alter the function and turnover of normal proteins. In the cardiac literature, oxidized phospholipids (eg, atherosclerosis in lipid-protein adducts) become dysfunctional and contribute to an immune response, promoting atherogenesis.[104-106]

In this work, a standardized approach to the evaluation of human tissue using the cSLO to image the LF pigments in the RPE is detailed and referred to as the MGS-FAF. Many studies in the literature lack sufficient standardization of technique and analysis for effective comparisons and conclusions.[72] The methodology reported in this thesis standardizes imaging technique and methodology while minimizing variability. Additionally, we are able to compare FAF images directly to high-resolution, digital, stereoscopic color fundus images. Such overlap studies will allow us to apply mathematical modeling systems, similar to the detailed description by Smith and coworkers.[75] The combined images are stored digitally and can be analyzed for future studies. Imaging techniques are constantly improving, and we anticipate that more reliable and reproducible technology will emerge. The ex vivo system allows us to use FAF beads or polymers that also will serve as an internal control reference for future studies, further improving our ability to quantify FAF of the RPE in eye bank eyes.

The next important step in standardization of the MGS-FAF is the careful size and location analysis that ensures that the area being tested is in the proper orientation (macula) and has the correct size relationship for repeatability and interspecimen comparison. The MGS-FAF utilizes the detailed macular localization techniques described in the MGS.[16] To summarize, there is a standardized size reference (1000-µm ruby sphere) that is also used in the MGS-FAF. This allows for accurate application of the grid template for determination of a reproducible surface area for measurement. The fovea is specifically localized in the MGS using proportional triangle method, and the accuracy follows in the MGS-FAF by using a color image overlay of the MGS onto the MGS-FAF (Figure 3). Rotational alignment is maintained by matching the peripapillary artifacts that are readily visible on both the MGS color image and the MGS-FAF grayscale image.

Calculation of the level of mean FAF is a function of the grayscale histogram over a given surface with the area measured in pixels. Since the input into the cSLO is standardized, the histogram should reflect a standardized, reproducible, and comparable value for large-scale study (intensity units). We eliminated areas of GA (hypofluorescent, values <38) and areas of bright light reflex (hyperfluorescent, values >250) from the calculations because they would artifactually change the mean FAF over a given surface area of viable RPE.

What is the role of LF in AMD? Many have proposed that oxidative mechanisms are involved in AMD progression.[21,23,27,36,37,57,59,61,66,105-107] Products of oxidation can be detected clinically as well as in donor eyes using the cSLO. Fundus autofluorescence is directly related to the presence of LF in the RPE, an oxidative product containing the primary fluorophore A2-E.[55] Evidence from clinical studies using the cSLO to study FAF has demonstrated that the level of FAF increases at the borders of GA in FAF, indicating that increasing FAF heralds the development of aAMD and subsequent vision loss.[55,76,79]

Detecting LF in vivo is possible using the cSLO. Rather than using a whole-image capture system (as in standard fundus photography), the cSLO uses *scanning* technology to image the macular region in a raster-like fashion, illuminating the fundus in a fraction of a second. Typically, cSLO captures 20 to 30 frames per second with each point being illuminated for less that 1 μs.[108] This rapid scanning is critical to obtain accurate images in vivo. The illuminating source for imaging is a laser or a collimated (parallel) beam of a single wavelength, making the final image more specific and sensitive for a given FAF compound, specifically LF. Also, the confocal technology permits localization of the imaged tissue to a specific cellular layer (RPE). Standard photographic techniques include all layers of the posterior pole that reflect or fluoresce.

A unique advantage of the MGS-FAF system is that all other chromophores are eliminated from the imaging process. For example, the cornea, lens, vitreous, and neurosensory retina are all removed so there is nothing except clear, optical lenses between the RPE and the cSLO. In a clinical setting, progressive nuclear cataract, macular luteal pigments, or vitreous opacities can add variability to FAF measurements. Additionally, the MGS-FAF allows for future biochemical analysis of the fresh (nonpreserved) RPE tissue.[109] Such analysis will allow for a direct clinical comparison of FAF to the biochemical makeup, including other fluorophores, beyond A2-E. In the future, other imaging techniques may allow for imaging of RPE morphology directly, such as confocal femtosecond laser imaging.

The MGS is a direct correlate to the AREDS and BDES with similar definitions. Therefore, drawing a direct link between a standardized methodology of FAF analysis and large-scale clinical and epidemiologic studies is extremely valuable. In essence, one is able to perform laboratory techniques on clinical phenotypes where the natural history has been well characterized.

This study has limitations. For example, Do fluorophores change immediately after death? Does the ambient light influence the FAF? Digital color stereoscopic images are taken immediately prior to the MGS-FAF images; would this affect the FAF? Is this responsible for the "ghost images" of retinal blood vessels (Figure 10)? Many of these variables are beyond our ability to control.

The recent discovery of advanced AMD with a variant in the gene coding for complement factor H[39-43] will help in our understanding of disease mechanisms, and the role of the complement system will improve our insights into disease mechanisms. Perhaps one day we will have a specific, early-stage therapy for those with this genetic variant. Most researchers feel that AMD has a multifactorial etiology, with many pathways involved in disease progression. In fact, what we refer to as AMD may be a final common pathway, seen as a typical clinical phenotype originating from a variety of differing etiologies. As we begin to understand the earlier events in pathologic aging, earlier targets for preventative therapy will emerge. The MGS-FAF allows us to compare early stages of AMD in eye bank eyes to age-matched controls. Eye bank tissue permits subsequent pathologic and biochemical analysis.

## CONCLUSIONS

This thesis describes a grading system (MGS) using FAF of the macula in eye bank eyes with all stages of AMD. The MGS-FAF uses a standardized methodology for image acquisition and analysis that eliminates many of the variables encountered with in vivo techniques. The system also enables simultaneous comparison of clinical phenotypes described in the AREDS to FAF. Future studies will enable researchers to analyze the tissue's biochemistry, proteome, genetics, and histolopathology and enable detection of early pathologic mechanisms occurring in AMD. Use of the cSLO allows precise tissue localization and reliable fluorophore excitation and detection. In 262 eyes selected for AMD analysis by the eye bank procurement team, the MGS-FAF did not demonstrate a significant association of mean FAF and age. Data generated in this study clearly show a statistically significant decline in MGS-FAF at MGS level 3 and a further decline at MGS level 4. The decline in FAF suggests an overall loss of RPE cells occurring in later stages of AMD. The higher levels of FAF in the early stages of AMD (MGS level 2) suggest that LF plays a role in the early pathogenesis of AMD. Future biochemical studies will be required to help understand the complex, early events that lead to vision loss in AMD.

### ACKNOWLEDGMENTS

Funding/Support: Supported by grant RO1-AG025392 from the National Institute on Aging, National Institutes of Health, and grant RO3-EY014176 from the National Eye Institute, National Institutes of Health; the Minnesota Lions Macular Degeneration Center, Minneapolis, Minnesota; University of Minnesota Vision Foundation, Minneapolis; and an Unrestricted grant from Research to Prevent Blindness Inc.

Financial Disclosures: None.

Conformity With Author Information: Exemption status for this study was obtained from the institutional review board at the University of Minnesota. All tissue was acquired with consent of the donor or donor family. The consent is in accordance with the principles outlined in the Declaration of Helsinki.

Other Acknowledgments: This work represents a compilation of efforts and intellectual input and hard work from the following: Xiao Feng, MD, and Adam Johnson, BS, who have put forth significant effort in data acquisition, and principle collaborator Deborah A. Ferrington, PhD, Cheryl Ethen, PhD, and Curt Nordgaard, MSc, who have all contributed to the proteomic work. I would like to recognize the University of Minnesota Department of Ophthalmology, and the Minnesota Lions Macular Degeneration Center. I also appreciate the continuous diligent work of the Minnesota Lions Eye Bank personnel as well as the tissue donors for providing valuable

research material used in this study. Without this support, these studies would not be possible. Next, I would like to recognize the Minnesota Lions who support this research in support of their mission to improve the vision of others. Finally, I wish to acknowledge the generous donors to our research program. Much of the equipment used in this study was from generous private contributions.

## REFERENCES

1. Buch H, Vinding T, La Cour M, Appleyard M, Jensen GB, Nielsen NV. Prevalence and causes of visual impairment and blindness among 9980 Scandinavian adults: The Copenhagen City Eye Study. *Ophthalmology* 2004;111:53-61.
2. Buch H, Vinding T, Nielsen NV. Prevalence and causes of visual impairment according to World Health Organization and United States criteria in an aged, urban Scandinavian population: the Copenhagen City Eye Study. *Ophthalmology* 2001;108:2347-2357.
3. Klaver CC, Wolfs RC, Vingerling JR, Hofman A, de Jong PT. Age-specific prevalence and causes of blindness and visual impairment in an older population: the Rotterdam Study. *Arch Ophthalmol* 1998;116:653-658.
4. O'Shea JG. Age-related macular degeneration: a leading cause of blindness [see comments]. *Med J Aust* 1996;165:561-564.
5. Mitchell P, Smith W, Attebo K, Wang JJ. Prevalence of age-related maculopathy in Australia. The Blue Mountains Eye Study. *Ophthalmology* 1995;102:1450-1460.
6. Klein R, Wang Q, Klein BE, Moss SE, Meuer SM. The relationship of age-related maculopathy, cataract, and glaucoma to visual acuity. *Invest Ophthalmol Vis Sci* 1995;36:182-191.
7. Klein R, Klein BE, Linton KL. Prevalence of age-related maculopathy. The Beaver Dam Eye Study. *Ophthalmology* 1992;99:933-943.
8. Hyman LG, Lilienfeld AM, Ferris FLd, Fine SL. Senile macular degeneration: a case-control study. *Am J Epidemiol* 1983;118:213-227.
9. Klein BE, Klein R. Cataracts and macular degeneration in older Americans. *Arch Ophthalmol* 1982;100:571-573.
10. Leibowitz HM, Krueger DE, Maunder LR, et al. The Framingham Eye Study monograph: an ophthalmological and epidemiological study of cataract, glaucoma, diabetic retinopathy, macular degeneration, and visual acuity in a general population of 2631 adults, 1973-1975. *Surv Ophthalmol* 1980;24:335-610.
11. Klein R. Overview of progress in the epidemiology of age-related macular degeneration. *Ophthalmic Epidemiol* 2007;14:184-187.
12. Wang JJ, Rochtchina E, Lee AJ, et al. Ten-year incidence and progression of age-related maculopathy: the Blue Mountains Eye Study. *Ophthalmology* 2007;114:92-98.
13. Topouzis F, Coleman AL, Harris A, et al. Prevalence of age-related macular degeneration in Greece: the Thessaloniki Eye Study. *Am J Ophthalmol* 2006;142:1076-1079.
14. Bandello F, Lafuma A, Berdeaux G. Public health impact of neovascular age-related macular degeneration treatments extrapolated from visual acuity. *Invest Ophthalmol Vis Sci* 2007;48:96-103.
15. The AREDS Group. A randomized, placebo-controlled, clinical trial of high-dose supplementation with vitamins C and E, beta carotene, and zinc for age-related macular degeneration and vision loss: AREDS report no. 8. *Arch Ophthalmol* 2001;119:1417-1436.
16. Olsen TW, Feng X. The Minnesota Grading System of eye bank eyes for age-related macular degeneration. *Invest Ophthalmol Vis Sci* 2004;45:4484-4490.
17. Ethen CM, Feng X, Olsen TW, Ferrington DA. Declines in arrestin and rhodopsin in the macula with progression of age-related macular degeneration. *Invest Ophthalmol Vis Sci* 2005;46:769-775.
18. Ethen CM, Reilly C, Feng X, Olsen TW, Ferrington DA. The proteome of central and peripheral retina with progression of age-related macular degeneration. *Invest Ophthalmol Vis Sci* 2006;47:2280-2290.
19. Kapphahn RJ, Giwa BM, Berg KM, et al. Retinal proteins modified by 4-hydroxynonenal: identification of molecular targets. *Exp Eye Res* 2006;83:165-175.
20. Nordgaard CL, Berg KM, Kapphahn RJ, et al. Proteomics of the retinal pigment epithelium reveals altered protein expression at progressive stages of age-related macular degeneration. *Invest Ophthalmol Vis Sci* 2006;47:815-822.
21. Decanini A, Nordgaard CL, Feng X, Ferrington DA, Olsen TW. Changes in select redox proteins of the retinal pigment epithelium in age-related macular degeneration. *Am J Ophthalmol* 2007;143:607-615.
22. Ethen CM, Hussong SA, Reilly C, Feng X, Olsen TW, Ferrington DA. Transformation of the proteasome with age-related macular degeneration. *FEBS Lett* 2007;581:885-890.
23. Ethen CM, Reilly C, Feng X, Olsen TW, Ferrington DA. Age-related macular degeneration and retinal protein modification by 4-hydroxy-2-nonenal. *Invest Ophthalmol Vis Sci* 2007;48:3469-3479.
24. Brown DM, Kaiser PK, Michels M, et al. Ranibizumab versus verteporfin for neovascular age-related macular degeneration. *N Engl J Med* 2006;355:1432-1444.
25. Gragoudas ES, Adamis AP, Cunningham ET Jr, Feinsod M, Guyer DR. Pegaptanib for neovascular age-related macular degeneration. *N Engl J Med* 2004;351:2805-2816.
26. Rosenfeld PJ, Brown DM, Heier JS, et al. Ranibizumab for neovascular age-related macular degeneration. *N Engl J Med* 2006;355:1419-1431.

27. Jiang S, Moriarty-Craige SE, Orr M, Cai J, Sternberg P Jr, Jones DP. Oxidant-induced apoptosis in human retinal pigment epithelial cells: dependence on extracellular redox state. *Invest Ophthalmol Vis Sci* 2005;46:1054-1061.
28. Yang P, Wiser JL, Peairs JJ, et al. Human RPE expression of cell survival factors. *Invest Ophthalmol Vis Sci* 2005;46:1755-1764.
29. Choudhary S, Xiao T, Srivastava S, et al. Toxicity and detoxification of lipid-derived aldehydes in cultured retinal pigmented epithelial cells. *Toxicol Appl Pharmacol* 2005;204:122-134.
30. Howes KA, Liu Y, Dunaief JL, et al. Receptor for advanced glycation end products and age-related macular degeneration. *Invest Ophthalmol Vis Sci* 2004;45:3713-3720.
31. Chen L, Wu W, Dentchev T, et al. Light damage induced changes in mouse retinal gene expression. *Exp Eye Res* 2004;79:239-247.
32. Takahashi A, Masuda A, Sun M, Centonze VE, Herman B. Oxidative stress-induced apoptosis is associated with alterations in mitochondrial caspase activity and Bcl-2-dependent alterations in mitochondrial pH (pHm). *Brain Res Bull* 2004;62:497-504.
33. Dunaief JL, Dentchev T, Ying GS, Milam AH. The role of apoptosis in age-related macular degeneration. *Arch Ophthalmol* 2002;120:1435-1442.
34. Age-Related Eye Disease Study Research G. A randomized, placebo-controlled, clinical trial of high-dose supplementation with vitamins C and E, beta carotene, and zinc for age-related macular degeneration and vision loss: AREDS report no. 8. *Arch Ophthalmol* 2001;119:1417-1436.
35. Beatty S, Koh H, Phil M, Henson D, Boulton M. The role of oxidative stress in the pathogenesis of age-related macular degeneration. *Surv Ophthalmol* 2000;45:115-134.
36. Cai J, Nelson KC, Wu M, Sternberg P Jr, Jones DP. Oxidative damage and protection of the RPE. *Prog Retin Eye Res* 2000;19:205-221.
37. Winkler BS, Boulton ME, Gottsch JD, Sternberg P. Oxidative damage and age-related macular degeneration. *Mol Vis*1999;5:32.
38. Justilien V, Pang JJ, Renganathan K, et al. SOD2 knockdown mouse model of early AMD. *Invest Ophthalmol Vis Sci* 2007;48:4407-4420.
39. Edwards AO, Ritter R 3rd, Abel KJ, Manning A, Panhuysen C, Farrer LA. Complement factor H polymorphism and age-related macular degeneration. *Science* 2005;308:421-424.
40. Hageman GS, Anderson DH, Johnson LV, et al. A common haplotype in the complement regulatory gene factor H (HF1/CFH) predisposes individuals to age-related macular degeneration. *Proc Natl Acad Sci U S A* 2005;102:7227-7232.
41. Haines JL, Hauser MA, Schmidt S, et al. Complement factor H variant increases the risk of age-related macular degeneration. *Science* 2005;308:419-421.
42. Klein RJ, Zeiss C, Chew EY, et al. Complement factor H polymorphism in age-related macular degeneration. *Science* 2005;308:385-389.
43. Zareparsi S, Branham KE, Li M, et al. Strong association of the Y402H variant in complement factor H at 1q32 with susceptibility to age-related macular degeneration. *Am J Hum Genet* 2005;77:149-153.
44. Rosenfeld PJ, Rich RM, Lalwani GA. Ranibizumab: phase III clinical trial results. *Ophthalmol Clin North Am* 2006;19:361-372.
45. Hardy J, Selkoe DJ. The amyloid hypothesis of Alzheimer's disease: progress and problems on the road to therapeutics. *Science* 2002;297:353-356.
46. Yi JJ, Ehlers MD. Ubiquitin and protein turnover in synapse function. *Neuron* 2005;47:629-632.
47. Gong B, Cao Z, Zheng P, et al. Ubiquitin hydrolase Uch-L1 rescues beta-amyloid-induced decreases in synaptic function and contextual memory. *Cell* 2006;126:775-788.
48. Feeney-Burns L, Berman ER, Rothman H. Lipofuscin of human retinal pigment epithelium. *Am J Ophthalmol* 1980;90:783-791.
49. Weiter JJ, Delori FC, Wing GL, Fitch KA. Retinal pigment epithelial lipofuscin and melanin and choroidal melanin in human eyes. *Invest Ophthalmol Vis Sci* 1986;27:145-152.
50. Kennedy CJ, Rakoczy PE, Constable IJ. Lipofuscin of the retinal pigment epithelium: a review. *Eye* 1995;9:763-771.
51. Dorey CK, Wu G, Ebenstein D, Garsd A, Weiter JJ. Cell loss in the aging retina. Relationship to lipofuscin accumulation and macular degeneration. *Invest Ophthalmol Vis Sci* 1989;30:1691-1699.
52. Katz ML, Gao CL, Rice LM. Formation of lipofuscin-like fluorophores by reaction of retinal with photoreceptor outer segments and liposomes. *Mech Ageing Dev* 1996;92:159-174.
53. Eldred GE. Age pigment structure. *Nature* 1993;364:396.
54. Eldred GE, Lasky MR. Retinal age pigments generated by self-assembling lysosomotropic detergents. *Nature* 1993;361:724-726.
55. Holz FG, Schutt F, Kopitz J, et al. Inhibition of lysosomal degradative functions in RPE cells by a retinoid component of lipofuscin. *Invest Ophthalmol Vis Sci* 1999;40:737-743.
56. Bergmann M, Schutt F, Holz FG, Kopitz J. Inhibition of the ATP-driven proton pump in RPE lysosomes by the major lipofuscin fluorophore A2-E may contribute to the pathogenesis of age-related macular degeneration. *FASEB J* 2004;18:562-564.
57. Boulton M, Dontsov A, Jarvis-Evans J, Ostrovsky M, Svistunenko D. Lipofuscin is a photoinducible free radical generator. *J Photochem Photobiol B* 1993;19:201-204.
58. Boulton M, Marshall J. Effects of increasing numbers of phagocytic inclusions on human retinal pigment epithelial cells in culture: a model for aging. *Br J Ophthalmol* 1986;70:808-815.

59. Davies S, Elliott MH, Floor E, et al. Photocytotoxicity of lipofuscin in human retinal pigment epithelial cells. *Free Radic Biol Med* 2001;31:256-265.
60. Godley BF, Shamsi FA, Liang FQ, Jarrett SG, Davies S, Boulton M. Blue light induces mitochondrial DNA damage and free radical production in epithelial cells. *J Biol Chem* 2005;280:21061-21066.
61. Kopitz J, Holz FG, Kaemmerer E, Schutt F. Lipids and lipid peroxidation products in the pathogenesis of age-related macular degeneration. *Biochimie* 2004;86:825-831.
62. Parish CA, Hashimoto M, Nakanishi K, Dillon J, Sparrow J. Isolation and one-step preparation of A2E and iso-A2E, fluorophores from human retinal pigment epithelium. *Proc Natl Acad Sci U S A* 1998;95:14609-14613.
63. Schutt F, Davies S, Kopitz J, Holz FG, Boulton ME. Photodamage to human RPE cells by A2-E, a retinoid component of lipofuscin. *Invest Ophthalmol Vis Sci* 2000;41:2303-2308.
64. Shamsi FA, Boulton M. Inhibition of RPE lysosomal and antioxidant activity by the age pigment lipofuscin. *Invest Ophthalmol Vis Sci* 2001;42:3041-3046.
65. Sparrow JR, Nakanishi K, Parish CA. The lipofuscin fluorophore A2E mediates blue light-induced damage to retinal pigmented epithelial cells. *Invest Ophthalmol Vis Sci* 2000;41:1981-1989.
66. Wassell J, Davies S, Bardsley W, Boulton M. The photoreactivity of the retinal age pigment lipofuscin. *J Biol Chem* 1999;274:23828-23832.
67. Boulton M, Rozanowska M, Rozanowski B. Retinal photodamage. *J Photochem Photobiol B* 2001;64:144-161.
68. Boulton M, Rozanowska M, Rozanowski B, Wess T. The photoreactivity of ocular lipofuscin. *Photochem Photobiol Sci* 2004;3:759-764.
69. Einbock W, Moessner A, Schnurrbusch UE, Holz FG, Wolf S. Changes in fundus autofluorescence in patients with age-related maculopathy. Correlation to visual function: a prospective study. *Graefes Arch Clin Exp Ophthalmol* 2005;243:300-305.
70. Feher J, Kovacs I, Artico M, Cavallotti C, Papale A, Balacco Gabrieli C. Mitochondrial alterations of retinal pigment epithelium in age-related macular degeneration. *Neurobiol Aging* 2006;27:983-993.
71. Holz FG, Bellmann C, Margaritidis M, Schutt F, Otto TP, Volcker HE. Patterns of increased in vivo fundus autofluorescence in the junctional zone of geographic atrophy of the retinal pigment epithelium associated with age-related macular degeneration. *Graefes Arch Clin Exp Ophthalmol* 1999;237:145-152.
72. Hopkins J, Walsh A, Chakravarthy U. Fundus autofluorescence in age-related macular degeneration: an epiphenomenon? *Invest Ophthalmol Vis Sci* 2006;47:2269-2271.
73. Hwang JC, Chan JW, Chang S, Smith RT. Predictive value of fundus autofluorescence for development of geographic atrophy in age-related macular degeneration. *Invest Ophthalmol Vis Sci* 2006;47:2655-2661.
74. Marmorstein AD, Marmorstein LY, Sakaguchi H, Hollyfield JG. Spectral profiling of autofluorescence associated with lipofuscin, Bruch's membrane, and sub-RPE deposits in normal and AMD eyes. *Invest Ophthalmol Vis Sci* 2002;43:2435-2441.
75. Smith RT, Chan JK, Busuoic M, Sivagnanavel V, Bird AC, Chong NV. Autofluorescence characteristics of early, atrophic, and high-risk fellow eyes in age-related macular degeneration. *Invest Ophthalmol Vis Sci* 2006;47:5495-5504.
76. Spaide RF. Fundus autofluorescence and age-related macular degeneration. *Ophthalmology* 2003;110:392-399.
77. Lois N, Owens SL, Coco R, Hopkins J, Fitzke FW, Bird AC. Fundus autofluorescence in patients with age-related macular degeneration and high risk of visual loss. *Am J Ophthalmol* 2002;133:341-349.
78. Schmitz-Valckenberg S, Bindewald-Wittich A, Dolar-Szczasny J, et al. Correlation between the area of increased autofluorescence surrounding geographic atrophy and disease progression in patients with AMD. *Invest Ophthalmol Vis Sci* 2006;47:2648-2654.
79. von Ruckmann A, Fitzke FW, Bird AC. Fundus autofluorescence in age-related macular disease imaged with a laser scanning ophthalmoscope. *Invest Ophthalmol Vis Sci* 1997;38:478-486.
80. Kim SR, Jang YP, Jockusch S, Fishkin NE, Turro NJ, Sparrow JR. The all-trans-retinal dimer series of lipofuscin pigments in retinal pigment epithelial cells in a recessive Stargardt disease model. *Proc Natl Acad Sci U S A* 2007;104:19273-19278.
81. Kim SR, He J, Yanase E, et al. Characterization of dihydro-A2PE: an intermediate in the A2E biosynthetic pathway. *Biochemistry* 2007;46:10122-10129.
82. Bellmann C, Holz FG, Schapp O, Volcker HE, Otto TP. [Topography of fundus autofluorescence with a new confocal scanning laser ophthalmoscope]. *Ophthalmologe* 1997;94:385-391.
83. von Ruckmann A, Fitzke FW, Bird AC. Distribution of fundus autofluorescence with a scanning laser ophthalmoscope. *Br J Ophthalmol* 1995;79:407-412.
84. Solbach U, Keilhauer C, Knabben H, Wolf S. Imaging of retinal autofluorescence in patients with age-related macular degeneration. *Retina* 1997;17:385-389.
85. Eldred GE, Katz ML. Fluorophores of the human retinal pigment epithelium: separation and spectral characterization. *Exp Eye Res* 1988;47:71-86.
86. Hammer M, Konigsdorffer E, Liebermann C, et al. Ocular fundus auto-fluorescence observations at different wavelengths in patients with age-related macular degeneration and diabetic retinopathy. *Graefes Arch Clin Exp Ophthalmol* 2008;246:105-114.
87. McBain VA, Townend J, Lois N. Fundus autofluorescence in exudative age-related macular degeneration. *Br J Ophthalmol* 2007;91:491-496.

88. Holz FG, Bindewald-Wittich A, Fleckenstein M, Dreyhaupt J, Scholl HP, Schmitz-Valckenberg S. Progression of geographic atrophy and impact of fundus autofluorescence patterns in age-related macular degeneration. *Am J Ophthalmol* 2007;143:463-472.
89. McBain VA, Townend J, Lois N. Fundus autofluorescence in exudative age-related macular degeneration. *Br J Ophthalmol* 2007;91:491-496.
90. Boulton M, Docchio F, Dayhaw-Barker P, Ramponi R, Cubeddu R. Age-related changes in the morphology, absorption and fluorescence of melanosomes and lipofuscin granules of the retinal pigment epithelium. *Vision Res* 1990;30:1291-1303.
91. Delori FC, Dorey CK, Staurenghi G, Arend O, Goger DG, Weiter JJ. In vivo fluorescence of the ocular fundus exhibits retinal pigment epithelium lipofuscin characteristics. *Invest Ophthalmol Vis Sci* 1995;36:718-729.
92. Delori FC, Goger DG, Dorey CK. Age-related accumulation and spatial distribution of lipofuscin in RPE of normal subjects. *Invest Ophthalmol Vis Sci* 2001;42:1855-1866.
93. Feeney-Burns L, Hilderbrand ES, Eldridge S. Aging human RPE: morphometric analysis of macular, equatorial, and peripheral cells. *Invest Ophthalmol Vis Sci* 1984;25:195-200.
94. Rozanowska M, Pawlak A, Rozanowski B, et al. Age-related changes in the photoreactivity of retinal lipofuscin granules: role of chloroform-insoluble components. *Invest Ophthalmol Vis Sci* 2004;45:1052-1060.
95. Wing GL, Blanchard GC, Weiter JJ. The topography and age relationship of lipofuscin concentration in the retinal pigment epithelium. *Invest Ophthalmol Vis Sci* 1978;17:601-607.
96. Gray DA, Woulfe J. Lipofuscin and aging: a matter of toxic waste. *Sci Aging Knowledge Environ* 2005;2005:re1.
97. Feeney L. Lipofuscin and melanin of human retinal pigment epithelium. Fluorescence, enzyme cytochemical, and ultrastructural studies. *Invest Ophthalmol Vis Sci* 1978;17:583-600.
98. Feeney-Burns L, Gao CL, Berman ER. The fate of immunoreactive opsin following phagocytosis by pigment epithelium in human and monkey retinas. *Invest Ophthalmol Vis Sci* 1988;29:708-719.
99. Feeney-Burns L, Hilderbrand ES, Eldridge S. Aging human RPE: morphometric analysis of macular, equatorial, and peripheral cells. *Invest Ophthalmol Vis Sci* 1984;25:195-200.
100. Warburton S, Davis WE, Southwick K, et al. Proteomic and phototoxic characterization of melanolipofuscin: correlation to disease and model for its origin. *Mol Vis* 2007;13:318-329.
101. Berendschot TT, van Norren D. On the age dependency of the macular pigment optical density. *Exp Eye Res* 2005;81:602-609.
102. Malik KJ, Chen CD, Olsen TW. Stability of RNA from the retina and retinal pigment epithelium in a porcine model simulating human eye bank conditions. *Invest Ophthalmol Vis Sci* 2003;44:2730-2735.
103. Morimoto RI. Stress, aging, and neurodegenerative disease. *N Engl J Med* 2006;355:2254-2255.
104. Berliner JA, Subbanagounder G, Leitinger N, Watson AD, Vora D. Evidence for a role of phospholipid oxidation products in atherogenesis. *Trends Cardiovasc Med* 2001;11:142-147.
105. Berliner JA, Watson AD. A role for oxidized phospholipids in atherosclerosis. *N Engl J Med* 2005;353:9-11.
106. Leitinger N. Oxidized phospholipids as modulators of inflammation in atherosclerosis. *Curr Opin Lipidol* 2003;14:421-430.
107. Kaemmerer E, Schutt F, Krohne TU, Holz FG, Kopitz J. Effects of lipid peroxidation-related protein modifications on RPE lysosomal functions and POS phagocytosis. *Invest Ophthalmol Vis Sci* 2007;48:1342-1347.
108. Bartsch D, Freeman W. Scanning laser ophthalmoscopy. In: Ciulla T, Regillo C, Harris A, eds: *Retina and Optic Nerve Imaging.* Philadelphia: Lippincott Williams & Wilkins; 2003:59-76.
109. Johnson AC, Olsen TW, Marimanikkuppam SS, Ferrington DA. Identification and quantitation of lipofuscin fluorophores in human donor eyes. Poster presented at: ARVO Meeting; 2005; Fort Lauderdale, FL.